ADVANCED FUNCTIONAL MATERIALS

Electrophosphorescence from a Polymer Guest–Host System with an Iridium Complex as Guest: Förster Energy Transfer and Charge Trapping**

By *Xiong Gong*, *Jacek C. Ostrowski*, *Daniel Moses*,* *Guillermo C. Bazan*,* and *Alan J. Heeger*

We report high-efficiency green electrophosphorescent light-emitting diodes obtained by using tris[9,9-dihexyl-2-(phenyl-4′-(-pyridin-2″-yl))fluorene]iridium(III) ($Ir(DPPF)_3$) as the guest, and a blend of poly(vinylcarbazole) (PVK) with 2-*tert*-butylphenyl-5-biphenyl-1,3,4-oxadiazol (PBD) as the host. The electrophosphorescent emission is characteristic of $Ir(DPPF)_3$, with its maximum at 550 nm. An external quantum efficiency of 8 % photons per electron and luminous efficiency of 29 cd A^{-1}, with maximum brightness of 3500 cd m^{-2}, were achieved at 1 wt.-% concentration of $Ir(DPPF)_3$. The devices exhibited no emission from PVK or PBD, even at the lowest concentration of $Ir(DPPF)_3$ (0.1 wt.-%). The results indicate that Förster energy transfer plays a minor role in achieving high efficiencies in these devices. Direct charge trapping appears to be the main operating mechanism.

1. Introduction

The performance of organic and polymer light-emitting diodes (OLEDs and PLEDs) has improved dramatically in recent years. In these devices, the electron and hole are injected from opposite electrodes and combine to form either singlet or triplet excitons.[1] Since radiative decay of the triplet is forbidden (triplet emission is weakly allowed in the presence of spin–orbit coupling), 100 % efficiency of the singlet emission results in a maximum internal quantum efficiency of 25 % for electroluminescence. Experiments have shown, however, that in luminescent semiconducting polymers, the singlet cross-section is considerably larger than that of triplet (by a factor of 3–4).[2] As a result, internal electroluminescence quantum efficiencies as high as 50 % of the corresponding photoluminescence (PL) quantum efficiency have been reported.[3] By utilizing phosphorescent dyes, such as platinum and iridium organometallic emitters (the use of high atomic number metals implies relatively large spin–orbit coupling), the internal quantum efficiency can be, in principle, increased to 100 %. The organometallic emitters enhance the efficiency of intersystem crossing from the first singlet excited state to the lowest lying triplet state and thereby enable phosphorescence from the triplet states.

Triplet-harvesting green and red LEDs based on platinum and iridium complexes as the guests and smaller molecules as the hosts have demonstrated high efficiencies.[4–9] For example, an external quantum efficiency (QE_{ext}) of 19.2 % ph/el and luminous efficiency (LE) of 73 cd A^{-1} at a current density (j) of 0.55 mA cm^{-2} was reported by using "starburst" perfluorinated phenylenes as a hole- and exciton-blocking layer, hole-transport materials 4,4′-4″-tri(*N*-carbazolyl)triphenylamine as a host and tris(2-phenylpyridine)iridium(III) (Ir-$(ppy)_3$) as the phosphorescent guest for green light emission.[7]

Electrophosphorescent LEDs based on polymers as the host materials offer the specific advantage that they can be fabricated by processing the active materials from solution; i.e., by spin-casting, screen-printing, or inkjet-printing at room temperature.[10–17] Furthermore, polymer-based electrophosphorescence represents an important step toward a new generation of full-color displays. Kim and co-workers[11] reported a $QE_{ext} = 1.9$ % ph/el with a brightness of 2500 cd m^{-2} for an Ir-$(ppy)_3$-doped poly(vinylcarbazole) (PVK) device with 3-(4-biphenylyl)-4-phenyl-5-*tert*-butylphenyl-1,2,4-triazole (TAZ) as a hole-blocking layer. O'Brien et al.[12] reported PtOEP (2,3,7,8,12,13,17,18-octaethyl-21*H*,23*H*-porphyrinplatinum(II))-doped PFO (poly (9,9-dioctylfluorene)) devices with a maximum QE_{ext} of 3.5 % ph/el. Zhu et al.[14] reported a QE_{ext} of 5.1 % ph/el and LE of 12 cd A^{-1}, achieved by incorporating the phosphorescent guest, Ir$(Bu\text{-}ppy)_3$, into CN-PPP (poly(2-((6′-cyano-6′-methylheptyl)oxy)-1,4-phenylene) for green light emission.

Results from our laboratory demonstrated $QE_{ext} = 10$ % ph/el, LE = 36 cd A^{-1}, with brightness over 8300 cd m^{-2} for green

[*] Dr. D. Moses, Prof. G. C. Bazan, Dr. X. Gong, J. C. Ostrowski, Prof. A. J. Heeger
Center for Polymers and Organic Solids
University of California at Santa Barbara
Santa Barbara, CA 93106–5096 (USA)
E-mail: bazan@chem.ucsb.edu; moses@ipos.ucsb.edu
Prof. G. C. Bazan
Department of Chemistry and Materials Department
University of California at Santa Barbara (UCSB)
Santa Barbara, CA 93106 (USA)
Prof. A. J. Heeger
Department of Physics and Materials Department
University of California at Santa Barbara (UCSB)
Santa Barbara, CA 93106 (USA)

[**] This work was supported by the Mitsubishi Chemical Center for Advanced Materials at UCSB and the Air Force Office of Scientific Research through the MURI Center ("Polymeric Smart Skins"), Charles Lee, Program Officer. Synthesis of the iridium complexes was supported by a grant to G. Bazan from Kodak. X. Gong is grateful to Dr. Gang Yu of Dupont Displays for valuable discussion.

 DOI: 10.1002/adfm.200304334

emission and $QE_{ext} = 5\,\%$ ph/el, $LE = 7.2\ cd\,A^{-1}$, with brightness over 2700 $cd\,m^{-2}$ for red emission. These were achieved by adding different iridium complexes into a blend of PVK with 2-*tert*-butylphenyl-5-biphenyl-1,3,4-oxadiazol (PBD).[15,16] These high efficiencies demonstrate the advantages of using phosphorescent guests as emissive centers in PLEDs. However, the quantum efficiency of electrophosphorescent PLEDs is still relatively low compared to the results obtained from electrophosphorescent LEDs prepared by vapor deposition of small molecules. Hence, achieving high efficiency and brightness remains a challenge in polymer-based electrophosphorescent LEDs.

In electrophosphorescent LEDs, the electrons and holes are initially injected into the organic host transport materials, and then the excitation is transferred to the organometallic emitters producing the phosphorescent excited states.[18,19] This excitation transfer can occur by various mechanisms, including Förster and/or Dexter energy transfer from the host transport material to the metal–organic center. Alternatively, direct, sequential trapping of both electrons and holes on the metal–organic center can play a role.

In the Förster mechanism,[20,21] the dipole–dipole interaction results in efficient transfer of the singlet excited-state energy from the host to the guest. Förster energy transfer from the host to the guest can lead to lower self-absorption losses because of the red-shift of the emission relative to the absorption in the blends.[22,23] The rate (K_{FET}) of Förster energy transfer is given by

$$K_{FET} = \tau_d^{-1} (R_0 / R)^6 \quad (1)$$

where τ_d is the lifetime of the host in the absence of the guest, R is the distance between the host and guest, and R_0 is the characteristic Förster distance which is given by

$$R_0^6 = \alpha \int_0^\infty F_d(\nu)\, \varepsilon_a(\nu)\, \nu^{-4}\, d\nu \quad (2)$$

where α depends on the relative orientation of the host and the guest dipole moments, the quantum yield of the host in the absence of the guest, and the refraction of the medium; $F_d(\nu)$ and $\varepsilon_\alpha(\nu)$ are the fluorescence and extinction spectra of the host and guest, respectively. The efficiency of the Förster energy transfer is dependent on the spectral overlap between the host emission spectrum and the guest absorption spectrum. Typically, the maximum distance over which Förster energy transfer can occur is 30 ~ 50 Å.

Dexter energy transfer of a neutral exciton from the host to a neutral exciton on the guest requires direct quantum mechanical tunneling of electrons between the host and the guest. It is therefore a short-range process that requires separations of no more than a few Å. In addition to singlet–singlet energy transfer, the Dexter mechanism also allows triplet–triplet energy transfer.

Förster and Dexter energy transfer can occur simultaneously if the singlet (or triplet) in the host is resonant with the corresponding levels in the guest. Although the conditions for Förster energy transfer can be easily evaluated from the absorption and emission spectra, evaluation of the conditions for efficient Dexter transfer require knowledge of the absolute energies of the excited states. These energies are not available for most light-emitting polymers.[24]

In the electron and hole trapping mechanism,[25,26] an excited guest molecule is formed by the sequential trapping of a hole and then an electron onto the metal–organic complex. The hole- and electron-trapping mechanism is most favorable if the HOMO (highest occupied molecular orbital) level of the guest is above (closer to vacuum level) that of the host, and if the LUMO (lowest unoccupied molecular orbital) level of the guest is below (farther from vacuum level) that of the host. However, having both the HOMO and LUMO of the guest within the gap of the host is not required. If (for example) the HOMO of the guest is above that of the host, holes will be readily trapped to form a cationic excited state of the guest. This cationic excited state of the guest will then function as an electron trap. Charge trapping and localization onto the guest requires overlap of the molecular orbitals of the host and guest molecules.

The use of Förster and/or Dexter energy transfer from small molecules and semiconducting polymers as hosts to organometallic emitters has been suggested for improving the external quantum efficiency of electrophosphorescent OLEDs/PLEDs.[4–17] The PL data that show very efficient energy transfer, even at low concentrations of the organometallic emitter, argue against the importance of excitation transfer via the Dexter mechanism. Thus, the dominant mechanisms for PL and electroluminescence (EL) in polymers doped with organometallic emitters are Förster energy transfer and charge trapping.[15,18,27–30]

We report here the results obtained from blends using PVK with PBD as the host and tris[9,9-dihexyl-2-(phenyl-4′-(-pyridin-2″-yl))fluorene]iridium(III) ($Ir(DPPF)_3$) as the guest. The structures of all three molecules are shown in Scheme 1. PVK was selected as the host because of the good spectral overlap of the host emission and the guest absorption (to maximize R_0, see Eq. 1). PVK is known as a hole-transporting material, but it is not an electron-transporting material.[31–33] Thus, PBD was mixed with PVK to enable the host blend to transport both electrons and holes.[31] In this study, we report high efficiencies and high brightness from electrophosphorescent PLEDs based on efficient charge trapping. By using $Ir(DPPF)_3$ as the guest and the blend of PVK with PBD as the host, $QE_{ext} = 8\,\%$ ph/el

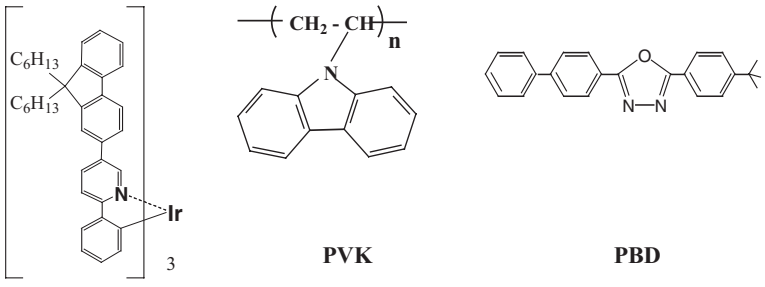

Scheme 1. Molecular structures of $Ir(DPPF)_3$, PVK, and PBD.

ADVANCED FUNCTIONAL MATERIALS

and LE= 29 cd A^{-1} were obtained at $j = 15$ mA cm^{-2}. The maximum brightness was over 3500 cd m^{-2} at 1 wt.-% $Ir(DPPF)_3$ concentration. No emission from PVK or PBD was observed from any devices containing $Ir(DPPF)_3$, even at 0.1 wt.-% concentration.

2. Results and Discussion

The UV-vis absorption spectra of thin films of pure $Ir(DPPF)_3$ and PVK–PBD (40 wt.-%) and the PL spectra of thin films of PVK–PBD (40 wt.-%) and pure $Ir(DPPF)_3$ are shown in Figure 1. Both the ligand–center and the metal–ligand charge transfer (MLCT) transitions are seen in the absorption spectrum of $Ir(DPPF)_3$: the peak around 340 nm is the absorption of the ligand–center, while the peaks at 410 nm and 440 nm are the absorption of the transition from the ground state to the singlet MLCT and triplet MLCT excited states. There is good overlap between the PL spectrum of PVK–PBD and the MLCT absorptions of $Ir(DPPF)_3$. Therefore, efficient Förster energy transfer from the PVK–PBD host[29,30] to the $Ir(DPPF)_3$ guest is expected. The presence of the heavy metal (iridium) in the complex ensures the fast intersystem crossing (ISC) to the triplet state in $Ir(DPPF)_3$ complex and subsequent emission from this state.[19]

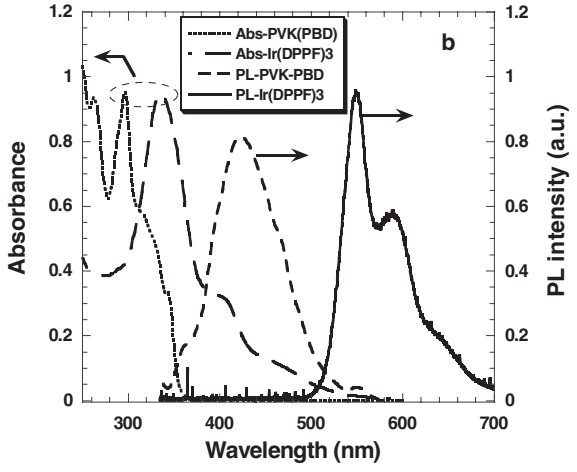

Fig. 1. Normalized absorption and photoluminescent spectra of thin films of $Ir(DPPF)_3$, PVK–PBD (40 wt.-%).

In order to test the efficiency of energy transfer, thin films of PVK–PBD (40 wt.-%) with different concentrations of $Ir(DPPF)_3$ were prepared and optically excited. The PL spectra of PVK–PBD (40 wt.-%) and PVK–PBD (40 wt.-%) with different concentrations of $Ir(DPPF)_3$ excited at 325 nm are shown in Figure 2. The PL profile contains two peaks: one centered at 425 nm, which results from the emission of the PVK–PBD host; and a second at 550 nm with a shoulder at 600 nm, which results from the $Ir(DPPF)_3$ triplet emission. The emission intensity at 425 nm reduced significantly as the $Ir(DPPF)_3$ concentration increased. At 8 wt.-% $Ir(DPPF)_3$, virtually no emission is observed from the host polymer; the $Ir(DPPF)_3$ emission completely dominates. Direct measurements of the

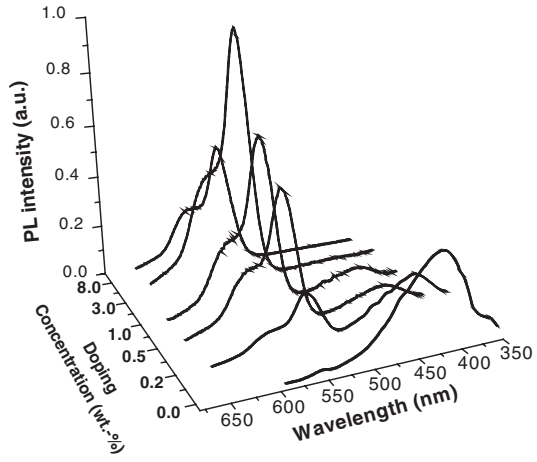

Fig. 2. Photoluminescent spectra of thin films of PVK–PBD (40 wt.-%) with different concentrations of $Ir(DPPF)_3$. All thin films had approximately the same thickness (100 nm).

optical absorption at 325 nm indicate that the absorption coefficient of PVK–PBD is ten times greater than that of pure $Ir(DPPF)_3$. Thus, for PVK–PBD:$Ir(DPPF)_3$, at least 90 % of the photons are absorbed by the PVK–PBD host polymer. Therefore, efficient Förster energy transfer from PVK–PBD to $Ir(DPPF)_3$ is confirmed by the dominant emission from the $Ir(DPPF)_3$.

The Förster energy transfer efficiency from PVK–PBD to $Ir(DPPF)_3$ can be written as

$$\eta = \frac{k_{FET}}{k_{FET}+\tau_d} = \frac{1}{1+(R_0/R)^6} \quad (3)$$

where K_{FET} and R_0 are from Equations 1 and 2, respectively.

Our goal here is to study how the Förster energy transfer efficiency depends on the $Ir(DPPF)_3$ concentration. The $Ir(DPPF)_3$ density, N_G, is given by

$$R = (N_G * \frac{4\pi}{3})^{-1/3} \quad (4)$$

Combining Equations 3 and 4, the energy transfer efficiency is given by

$$\eta = \frac{1}{1+\left[R_0/(N_G * \frac{4\pi}{3})^{-1/3}\right]^6} \quad (5)$$

All the thin films studies had approximately the same thickness and were optically excited under the same conditions. Moreover, all films had identical absorption and PL spectra. Thus, α, $F_d(\nu)$ and $\varepsilon_\alpha(\nu)$ in Equation 2 can be assumed to be constant, which results in a constant R_0 for all the films with different $Ir(DPPF)_3$ concentrations. In studies of conjugated polymer blends, a value of $R_0 \approx 30$ Å was obtained from time-resolved studies of Förster excitation transfer.[34] However, the precise value of R_0 has not yet been determined for the system studied here. Therefore, the relative energy transfer efficiency can be predicted either as a function of $Ir(DPPF)_3$ concentration or, equivalently, the distance between the host and the

guest. The results are shown in Figure 3. At lower $Ir(DPPF)_3$ concentrations, the energy transfer from the PVK–PBD to $Ir(DPPF)_3$ was incomplete because the average distance from a photoexcited polymer chain to the nearest $Ir(DPPF)_3$ is too large ($R > R_0$).[10] At higher concentrations ($R < R_0$), all energy

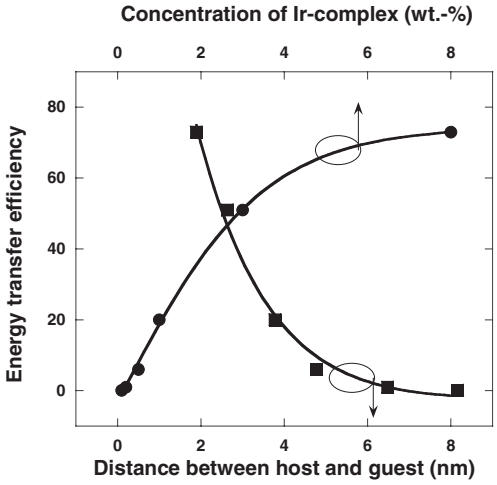

Fig. 3. Relative energy transfer efficiency as a function of $Ir(DPPF)_3$ concentration and the distance between the host and the guest (marks represent the calculated values, dashed lines represent the fitted curves).

was transferred to $Ir(DPPF)_3$, but the emission efficiency was evidently reduced by concentration quenching. We also found that the PL of neat $Ir(DPPF)_3$ film is very weak. These results indicate efficient Förster energy transfer from PVK–PBD to $Ir(DPPF)_3$ even at concentrations less than 3 wt.-% of $Ir(DPPF)_3$; significantly lower than that (8 wt.-%) reported for $Ir(ppy)_3$ in PVK.[11]

The EL spectra of the devices made from different concentrations of $Ir(DPPF)_3$ only show the characteristic spectrum of $Ir(DPPF)_3$, with one peak at 550 nm and another at 600 nm. There is no emission of PVK or PBD from any devices containing $Ir(DPPF)_3$, even at 0.1 wt.-% guest concentration. The EL spectra of the device made from 0.1 wt.-% doping concentration of $Ir(DPPF)_3$ at different applied voltages are shown in Figure 4. Note that the concentration required to completely quench the PVK–PBD (40 wt.-%) PL emission was 8 wt.-% of

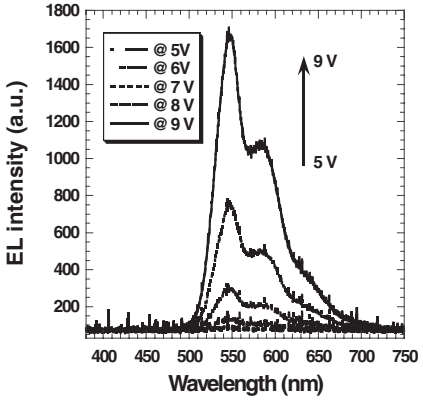

Fig. 4. Electroluminescent spectra of LEDs made from PVK–PBD (40 wt.-%) with 0.1 wt.-% $Ir(DPPF)_3$ concentration at different applied voltages.

$Ir(DPPF)_3$. The absence of PVK or PBD EL emission from the devices contained the $Ir(DPPF)_3$, even at the lowest concentration of $Ir(DPPF)_3$ (0.1 wt.-%) is consistent with charge trapping on the Ir-complex (rather than Förster transfer) as the dominant mechanism in the LEDs. We conclude, therefore, that the iridium complex traps both electrons and holes, which enables the direct recombination of holes and electrons via the Ir complex. If energy transfer were the dominant EL mechanism, the EL emission of PVK or PVK–PBD would be expected to appear when the triplet of $Ir(DPPF)_3$ becomes saturated, i.e., at higher applied voltages and lower concentrations.[12,19] Similar "charge trapping" has been observed in PVK–PBD doped with Ir complexes.[9,13,15,16] and in a conjugated polymer doped with an Ir complex.[17]

Since the $Ir(DPPF)_3$ complex functions as both a hole trap and an electron trap, the HOMO and/or the LUMO of the Ir complex must fall within the bandgap of the polymer. The HOMO and LUMO of PVK are –5.4 eV and –1.9 eV, respectively.[33] The HOMO and LUMO of $Ir(DPPF)_3$ are –4.82 eV and –1.69 eV, as determined by cyclic voltammetry. Hence, the HOMO of $Ir(DPPF)_3$ is 0.58 eV above that of the PVK, implying that holes are readily trapped on the $Ir(DPPF)_3$. Assuming, therefore, that the HOMO functions as the hole trap, the electron can subsequently hop onto the $Ir(DPPF)_3^+$ to form the triplet excited state. Therefore, the dominant mechanism in electrophosphorescent PLEDs is charge trapping followed by electron–hole recombination on the organometallic emitter.

Figure 5 depicts the current density versus voltage and the brightness versus voltage characteristics of a device made from PVK–PBD (40 wt.-%) with 1 wt.-% concentration of

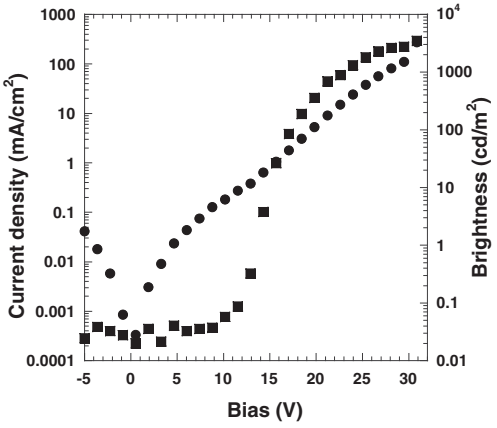

Fig. 5. Brightness and current density characteristics of the ITO/PEDOT/PVK–PBD: $Ir(DPPF)_3$/Ca/Ag device with 1 wt.-% $Ir(DPPF)_3$ concentration as functions of applied voltage.

$Ir(DPPF)_3$. The device turns on at ~10 V and has maximum brightness (at 30 V) greater than 3500 cd m^{-2}.

To evaluate the efficiencies, the devices were fabricated with different concentrations of $Ir(DPPF)_3$. Figure 6 shows the LE [cd A^{-1}] and power efficiency [lumens W^{-1}] versus the current density (mA cm^{-2}) for devices with 1 wt.-% $Ir(DPPF)_3$. The maximum LE = 29 cd A^{-1} and highest power efficiency = 3.3 lumens W^{-1} were obtained with 1 wt.-% concentration of $Ir(DPPF)_3$. The inset to Figure 6 shows QE_{ext} as a function of

ADVANCED FUNCTIONAL MATERIALS

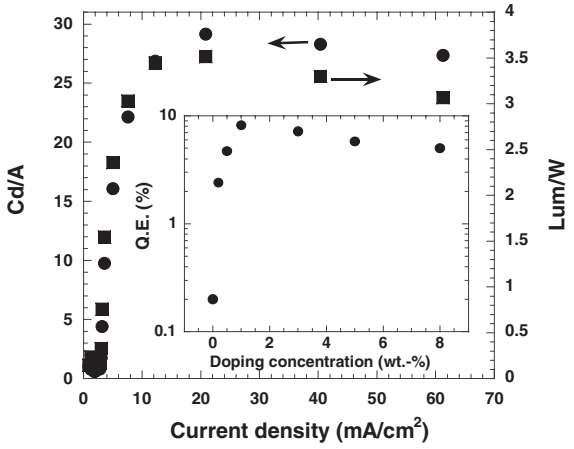

Fig. 6. Luminous efficiencies [cd A^{-1}] and power efficiencies [lumens W^{-1}] versus current density [mA cm^{-2}] of $Ir(DPPF)_3$/PVK–PBD (40 wt.-%) LEDs with 1 wt.-% $Ir(DPPF)_3$ concentration. Inset: External quantum efficiencies (QE_{ext}) of the ITO/PEDOT/PVK–PBD:$Ir(DPPF)_3$/Ca/Ag devices versus $Ir(DPPF)_3$ concentration [wt.-%] at the constant current density of 15 mA cm^{-2}.

$Ir(DPPF)_3$ concentration. At the low concentrations, QE_{ext} increased with increasing concentrations of $Ir(DPPF)_3$. At high concentrations, QE_{ext} decreased, probably due to the triplet–triplet annihilation on the $Ir(DPPF)_3$.[7,18,27] The maximum $QE_{ext} = 8\,\%$ ph/el (at $j = 15$ mA cm^{-2}) was at 1 wt.-% $Ir(DPPF)_3$, i.e., much lower than that reported for $Ir(ppy)_3$ in PVK devices.[11]

3. Conclusions

We have demonstrated high-efficiency green electroluminescence based on efficient charge trapping on a metal–organic complex. The EL spectra show the characteristic spectrum of $Ir(DPPF)_3$ with one peak at 550 nm and another at 600 nm. Efficient electrophosphorescence with $QE_{ext} = 8\,\%$ ph/el and LE = 29 cd A^{-1} was obtained by using $Ir(DPPF)_3$ as the guest and a PVK–PBD blend as the host. The maximum brightness was over 3500 cd m^{-2} at 1 wt.-% $Ir(DPPF)_3$. No EL emission from the PVK–PBD was evident, even at only 0.1 wt.-% $Ir(DPPF)_3$. The results indicate that Förster energy transfer plays a minor role in achieving high efficiencies in these devices. Direct charge trapping on the $Ir(DPPF)_3$ guest appears to be the main operating mechanism. More generally, the data demonstrate that high-efficiency electrophosphorescent LEDs are possible with a polymer as the host and a heavy-metal complex as the guest, and that these devices can be fabricated by simple and low-cost processes consistent with inkjet-printing and screen-printing techniques.

4. Experimental

The synthesis and characterization of $Ir(DPPF)_3$ have been reported elsewhere [35]. PVK and PBD were obtained from Aldrich and used without further purification. The molecular structures of PVK, PBD, and $Ir(DPPF)_3$ are shown in Scheme 1. For spectroscopy measurements, thin films were prepared by spin-casting from solution (dichloroethane as solvent) on quartz substrates. The UV-vis absorption spectra were measured on a Shimadzu UV-2401PC UV-vis recording spectrophotometer. Photoluminescence (PL) spectra were measured on a Spex Fluoromax-2 spectrometer.

For device fabrication, we employed only the single active-layer configuration with poly(3,4-ethylene dioxythiophene):poly(styrene sulfonic acid) (PEDOT:PSS) on indium tin oxide (ITO) as the hole-injecting bilayer electrode. The device configuration is (ITO)/PEDOT:PSS/PVK–PBD:$Ir(DPPF)_3$/Ca/Ag, as shown schematically in Figure 7. PEDOT:PSS was spin-cast onto ITO surface. The emitting layer, polymers with different concentrations of Ir complexes, were then spun onto the PEDOT:PSS layer. Film thicknesses were around 100 nm. The Ca/Ag cathode was deposited through a shadow mask by thermal evaporation at 4×10^{-7} torr.

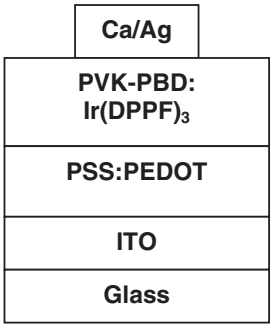

Fig. 7. Device configuration.

The current–voltage and brightness–voltage characteristics were measured using a Keithley 236 source measurement unit and a calibrated silicon photodiode [10,36] (computer interfaced with LabView supplied by National Instruments). The electroluminescent spectra were measured with a single-grating monochromator equipped with a photometric charge-coupled device (CCD) camera as the detector. All device fabrication and testing were carried out in a controlled atmosphere dry-box in N_2 atmosphere.

Received: January 16, 2003
Final version: February 24, 2003

[1] A. R. Brown, K. Pichler, N. C. Greenham, D. D. C. Bradley, R. H. Friend, A. B. Holmes, *Chem. Phys. Lett.* **1993**, *210*, 61.
[2] M. Wohlgenannt, K. Tandon, S. Mazumdar, S. Ramasesha, Z. V. Vardeny. *Nature* **2001**, *409*, 494.
[3] Y. Cao, I. D. Parker, G. Yu, C. Zhang, A. J. Heeger, *Nature* **1999**, *397*, 414.
[4] M. A. Baldo, M. E. Thompson, S. R. Forrest, *Nature* **2000**, *403*, 750.
[5] T. Tsutsui, M. J. Yang, M. Yahiro, K. Nakamura, T. Watanabe, T. Tsuji, Y. Fukuda, T. Wakimoto, S. Miyaguchi, *Jpn. J. Appl. Phys.* **1999**, *38*, L1502.
[6] C. Adachi, M. A. Baldo, S. R. Forrest, *Appl. Phys. Lett.* **2000**, *77*, 904.
[7] M. Ikai, S. Tokito, Y. Sakamoto, T. Suzuki, Y. Taga, *Appl. Phys. Lett.* **2001**, *79*, 156.
[8] C. Adachi, M. A. Baldo, M. E. Thompson, S. R. Forrest, *J. Appl. Phys.* **2001**, *90*, 5048.
[9] S. Lamansky, P. Djurovich, D. Murphy, F. Abdel-Razzaq, H. E. Lee, C. Adachi, P. E. Burrows, S. R. Forrest, M. E. Thompson, *J. Am. Chem. Soc.* **2001**, *123*, 4304.
[10] M. D. McGehee, T. Bergstedt, C. Zhang, A. P. Saab, M. B. O'Regan, G. C. Bazan, V. I. Srdanov, A. J. Heeger, *Adv. Mater.* **1999**, *11*, 1349.
[11] C. L. Lee, K. B. Lee, J. J. Kim, *Appl. Phys. Lett.* **2000**, *77*, 2280.
[12] D. F. O'Brien, C. Giebler, R. B. Fletcher, J. Cadlby, L. C. Palilis, D. G. Lidzey, P. A. Lane, D. C. Bradley, W. Blau, *Synth. Met.* **2001**, *116*, 379.
[13] S. Lamansky, R. C. Kwong, M. Nugent, P. I. Djurovich, M. E. Thompson, *Org. Electron.* **2001**, *2*, 53.
[14] W. G. Zhu, Y. Q. Mo, M. Yuan, W. Yang, Y. Cao, *Appl. Phys. Lett.* **2002**, *80*, 2045.
[15] X. Gong, M. R. Robinson, J. C. Ostrowski, D. Moses, G. C. Bazan, A. J. Heeger, *Adv. Mater.* **2002**, *14*, 581.
[16] X. Gong, J. C. Ostrowski, D. Moses, G. C. Bazan, A. J. Heeger, *Appl. Phys. Lett.* **2002**, *81*, 3711.
[17] X. Gong, J. C. Ostrowski, D. Moses, G. C. Bazan, A. J. Heeger, M. S. Liu, A. K-Y. Jen, *Adv. Mater.* **2003**, *15*, 45.
[18] I. H. Campbell, D. L. Smith, S. Tretiak, R. L. Martin, C. J. Neef, J. P. Ferraris, *Phys. Rev. B* **2002**, *65*, 085 210.
[19] a) M. A. Baldo, S. R. Forrest, *Phys. Rev. B* **2000**, *62*, 10 958. b) M. A. Baldo, S. R. Forrest, *Phys. Rev.* **2000**, *B62*, 10 967.

[20] T. Förster, *Discuss. Faraday Soc.* **1959**, *7*, 27.
[21] D. L. Dexter, *J. Chem. Phys.* **1953**, *21*, 836.
[22] R. Gupta, M. Stevenson, A. Dogariu, H. Wang, M. D. McGehee, J. Y. Park, V. Srdanov, A. J. Heeger, *Appl. Phys. Lett.* **1998**, *73*, 3492.
[23] R. Gupta, M. Stevenson, A. J. Heeger, *J. Appl. Phys.* **2002**, *92*, 4874.
[24] A. P. Monkman, H. D. Burrow, L. J. Hartwell, L. E. Horsburgh, I. Hamblett, S. Navaratnam, *Phys. Rev. Lett.* **2001**, *86*, 1358.
[25] K. Utsugi, S. Takano, *J. Electrochem. Soc.* **1992**, *139*, 3610.
[26] H. Suzuki, A. Hoshino, *J. Appl. Phys.* **1996**, *79*, 8816.
[27] P. A. Lane, L. C. Palilis, D. F. O'Brien, C. Giebeler, A. J. Cadby, D. G. Lidzey, A. J. Campbell, W. Blau, D. D. C. Bradley, *Phys. Rev.* **2001**, *B63*, 2 352 061.
[28] J. Kalinowski, W. Stampor, J. Mezyk, M. Cocchi, D. Virgili, V. Fattori, P. Di Marco, *Phys. Rev.* **2002**, *B66*, 2 353 211.
[29] X. Gong, S. H. Lim, J. C. Ostrowski, C. J. Bardeen, G. C. Bazan, D. Moses, A. J. Heeger, unpublished.
[30] R. A. Negres, X. Gong, J. C. Ostrowski, D. Moses, G. C. Bazan, A. J. Heeger, unpublished.
[31] J. Kido, K. Hongawa, K. Okuyama, K. Nagai, *Appl. Phys. Lett.* **1993**, *63*, 2627.
[32] C. Zhang, H. von Seggern, K. Pakbaz, B. Kraabel, H.-W. Schmidt, A. J. Heeger, *Synth. Met.* **1994**, *62*, 35.
[33] *Organic Electroluminescent Materials and Devices* (Ed: S. Muyata), Gordon and Breach, Newark, NJ **1997**, p. 218.
[34] A. Dogariu, R. Gupta, A. J. Heeger, H. L. Wang, *Synth. Met.* **1999**, *100*, 95.
[35] J. C. Ostrowski, M. R. Robinson, A. J. Heeger, G. C. Bazan, *Chem. Commun.* **2002**, *7*, 784.
[36] J. Gao, Y. F. Li, G. Yu, A. J. Heeger, *J. Appl. Phys.* **1999**, *86*, 4594.

